

Quantification of Soil Permanganate Oxidizable C (POXC) Using Infrared Spectroscopy

Francisco J. Calderón*

Central Great Plains Research Station
USDA-ARS
Akron, CO 80720

Steve Culman

School of Environ. and Natural Resources
Ohio State Univ.
Wooster, OH 44691

Johan Six

Dep. of Environmental Systems Science
Swiss Federal Institute of Technology
Zurich

Alan J. Franzluebbers

Plant Science Research
USDA-ARS
Raleigh, NC 27695

Meagan Schipanski

Soil and Crop Sciences
Colorado State Univ.
Fort Collins, CO 80523

Joshua Beniston

Santa Rosa Junior College
Santa Rosa, CA 95401

Stuart Grandy

Dep. of Natural Resources and the Environ.
Univ. of New Hampshire
Durham, NH 03824

Angela Y. Y. Kong

Center for Climate Systems Research
Columbia Univ.
New York, NY 10027

Labile soil carbon is an important component of soil organic matter because it embodies the mineralizable material that is associated with short-term fertility. Permanganate-oxidizable C (POXC) is a widely used method for the study of labile C dynamics in soils. Rapid methods are needed to measure labile C, and better understand how this pool varies with soil C at regional scales. Infrared spectroscopy is an inexpensive way to quantify SOC and observe fluctuations in C functional groups. Using a sample set that encompassed several soil types and plant communities (seven different research projects, $n = 496$), soils were analyzed via diffuse reflectance Fourier transformed mid-infrared (MidIR, 4000–400 cm^{-1}) and near-infrared (NIR, 10000–4000 cm^{-1}) spectroscopy. Spectral data were used to develop calibrations for POXC, soil organic C (SOC), and total N (TN) using partial least squares (PLS) regression. The MidIR predicted POXC slightly better than the NIR, with calibration and/or validation R^2 values ranging from 0.77 to 0.81 depending on spectral pretreatments. Predictions for POXC were better than SOC and TN, but site variability influenced the calibration quality for SOC and TN. Using a selected MidIR region, which included bands correlated to POXC (3225–2270 cm^{-1}), reduced the calibration quality, but still gave acceptable R^2 values of 0.76 to 0.77 for the calibration and validation sets. We show that POXC can be predicted using NIR and MidIR spectra. Selecting informative spectral bands offers an alternative to using full spectra for PLS regressions.

Abbreviations: LFL, Living Field Laboratory; LTRAS, Long-Term Research on Agricultural Systems; MidIR, diffuse reflectance Fourier transformed mid-infrared spectroscopy; MSC, multiplicative scatter correction; OUG, Ohio Urban Garden; NIR, diffuse reflectance Fourier transformed near-infrared spectroscopy; PLS, partial least squares; PCA, principal components analysis; POXC, permanganate-oxidizable carbon; RMSE, root mean squared error; SOC, soil organic C; SNV, standard normal variate; TN, total soil N.

One of the most important aspects of agricultural soil quality pertains to the soil's capacity to cycle nutrients and make them available to growing crops. Permanganate oxidizable C reflects a fraction of labile soil C that has been related to soil microbial biomass and particulate organic C, which are fundamental for soil C cycling (Culman et al., 2012). Also, POXC has been shown to be sensitive to changes in management as well as environmental conditions (de Moraes Sá et al., 2014; Margenot et al., 2015; Panettieri et al., 2015; Plaza-Bonilla et al., 2014; Xiang et al., 2015), sometimes more so than total soil C (Wang et al., 2014). The POXC is often, but not always, correlated to total soil C content (Lucas and Weil, 2012; Veum et al., 2014). Furthermore, POXC is a frac-

Disclaimer: The use of trade, firm, or corporation names is for the information and convenience of the reader. Such use does not constitute an official endorsement or approval by the USDA or the Agricultural Research Service of any product or service to the exclusion of others that may be suitable. The USDA prohibits discrimination in all its programs and activities on the basis of race, color, national origin, age, disability, and where applicable, sex, marital status, familial status, parental status, religion, sexual orientation, genetic information, political beliefs, reprisal, or because all or part of an individual's income is derived from any public assistance program.

Soil Sci. Soc. Am. J. 81:277–288
doi:10.2136/sssaj2016.07.0216
Received 15 July 2016.
Accepted 1 Dec. 2016.

*Corresponding author: (francisco.calderon@ars.usda.gov).

© Soil Science Society of America, 5585 Guilford Rd., Madison WI 53711 USA. All Rights reserved.

Core Ideas:

- Infrared spectroscopy and chemometrics can be used to quantify soil labile C.
- Soils amended with organic materials need to be taken into account during calibration development.
- Selection of spectral regions can give parsimonious predictions of soil total and labile C.

tion of total soil C that is thought to be easily degradable by soil microbes and is also an important source of mineralizable N and P for growing crops.

Diffuse reflectance mid-infrared (MidIR) and near-infrared (NIR) spectroscopy offer an alternative to traditional wet chemistry-based soil analyses because they are inexpensive, high-throughput, and require minimal sample preparation. The use of spectra from whole soils is desirable given that the only sample preparation needed before presentation to the instrument is drying and uniform grinding (Reeves, 2003). The MidIR spectral region encompasses fundamental overtone absorbance bands from several organic and mineral functional groups such as C=C, Si–O, C–H, O–H, N–H, and C–N among others (Parikh et al., 2014; Reeves et al., 2012). In contrast, the NIR spectral region is largely made up of overtones, combination, and harmonics of C–H, N–H, and O–H vibrations. Spectral interpretation is more straightforward for the MidIR compared to the NIR due to the nature of the absorbance bands in each region (Parikh et al., 2014). Chemometric methods are necessary to obtain quantitative information from the large amount of data contained in MidIR and NIR spectra (Bellon-Maurel and McBratney, 2011; Reeves et al., 2006, 2012; Stenberg et al., 2010). Previous work has shown that it is feasible to build reliable calibrations based on heterogeneous soil samples provided that the spectral and analyte data sets bracket the variation in the target samples (Reeves et al., 2006). Even though the NIR and MidIR spectral regions differ significantly at the theoretical level, soil properties that give good calibrations with NIR tend to calibrate well using MidIR spectral data (Madari et al., 2005; Reeves, 2010). On occasion, however, one of the spectral regions outperforms the other depending on the soil property being quantified (Viscarra Rossel et al., 2006). Besides using the full spectral range, spectral region selection can be a useful strategy in calibration development, because the smaller number of spectral data points can lead to more time efficient and parsimonious multivariate models (Fang et al., 2015).

Rapid and inexpensive methods are needed to assess soil constituents and labile SOC. A previous study showed that photacoustic Fourier transform infrared spectroscopy data can be used to accurately predict labile C determined by incubation and curve fitting (Peltre et al., 2014). Similarly, Thomsen et al. (2009) showed that NIR can be used to assess C lability as determined by NaOCl oxidation. Veum et al. (2014) used MidIR and NIR spectra from demineralized samples to predict POXC in soils from Missouri, USA. A more comprehensive study is needed to ascertain the potential of infrared spectra of whole soils to predict labile C, as a proxy for soil quality, in a wider geographic context. Our objectives were to (i) determine if MidIR and NIR could be used to determine POXC, SOC, and TN on a wide range of soils, (ii) compare the calibration quality of the MidIR and NIR, and (iii) test if a specific spectral regions can be used instead of the full MidIR spectrum to develop more parsimonious calibrations for POXC.

MATERIALS AND METHODS

Soils

Samples included in the study came from seven different agricultural research projects with a total number of samples of 496 (Table 1). The W.K. Kellogg Biological Station (KBS) site was located in Hickory Corners, MI (42°24' N, 85°22' W), on Kalamazoo (fine-loamy, mixed, mesic Typic Hapludalfs) and Oshtemo (coarse-loamy, mixed, mesic Typic Hapludalfs) soil series. The Long-Term Research on Agricultural Systems (LTRAS; currently known as the Russell Ranch Sustainable Agriculture Facility) site was located in Winters, CA (38°36' N, 121°50' W) on a Yolo silt loam (fine-silty, mixed nonacid, thermic Typic Xerorthents) and Rincon silty clay loam (fine, montmorillonitic, thermic Mollic Haploxeralfs). The Niles site was located in Niles, KS (38°58' N, 97°28' W) on a Geary silt loam (fine-silty, mixed, superactive, mesic Udic Argiustolls). The NY-Grain site was located in Seneca and Yates Counties, NY (42°39' to 42°44' N, 77°04' to 76°43' W) on sandy clay loams, silt loams, and clay loams (mixed, active Hapludalfs). The Watkinsville site was located in Watkinsville, GA (33°52' N, 83°25' W) on Cecil–Madison–Pacolet (fine, kaolinitic, thermic Typic Kanhapludult) soil series with sandy loam, loam, or sandy clay loam surface textures. The Ohio Urban Garden (OUG) samples came from urban vacant lots in Youngstown, OH (41°04' N, 80°40' W). The soils were obtained from an experiment testing the use of organic amendments, which included unamended soils, compost amended soils, as well as compost-biochar combinations (Beniston et al., 2015). The Living Field Laboratory (LFL) project was established in 1993 to examine the effect of cover crops on corn rotations at the KBS site (42°24' N, 85°24' W, 288 m a.s.l.) on sandy loam Haplic Luvisols (Snapp et al., 2010). All samples were collected, composited and air-dried immediately. Sampling dates and depth varied by study, as outlined in the references listed in Table 1.

Permanganate oxidizable C analyses were based on the laboratory procedures and calculations of Weil et al. (2003). Briefly, 2.5 g of soil were mixed with 18 mL of deionized water and 2 mL of 0.2 M KMnO_4 solution. The mixtures were shaken for 2 min at 240 oscillations per minute. Samples were allowed to settle for 10 min., after which 0.5 mL of the supernatant was mixed with 49.5 mL of deionized water. Then, 200 mL of each sample was loaded into a 96-well plate containing a set of KMnO_4 standards. Absorbance was measured at 550 nm with a SpectraMax M5 (Molecular Devices, Sunnyvale, CA). Total SOC and TN were measured with a direct combustion analyzer, as detailed in Culman et al. (2012).

Infrared Spectroscopy

Diffuse reflectance mid-infrared and NIR calibrations were performed with spectra from neat soil samples, not diluted with KBr (Reeves et al., 2001). The samples were ground with a mortar and pestle, then dried at 60°C overnight before scanning. The dried and ground samples were scanned using a Pike AutoDIFF diffuse reflectance accessory (Pike Technologies, Madison, WI)

in line with a Digilab FTS 7000 spectrometer (Varian, Inc., Palo Alto, CA). Potassium bromide and sulfur were used as background samples for the MidIR and NIR, respectively. A quartz beam splitter and lead selenide detector were used for the NIR scans, and a KBr beam splitter and deuterated triglycine sulfate detector were used for the MidIR scans. Each spectrum consisted of 64 co-added scans from 10,000 to 4000 cm^{-1} for the NIR and 4000 to 400 cm^{-1} for the MidIR. The NIR spectra are made up of 3113 data points, and the MidIR spectra have 1868 data points. All spectral data were collected as pseudo-absorbance, referred to as absorbance throughout the text. Organic band assignments follow Parikh et al. (2014) unless otherwise specified.

Correlation of Spectral and Analyte Data

A correlation analysis was performed to identify which spectral bands are more informational in regards to the POXC, SOC, and TN. Before the correlation analysis, the MidIR and NIR spectral data were baseline corrected using the baseline offset feature of Unscrambler 10.3 (Camo Software, Oslo, Norway). Then the Pearson correlation coefficient (R) between the baseline corrected spectral data and the POXC, SOC, and TN data were calculated with the *correl* function of Microsoft Excel 2007.

Principal Components Analysis

To examine the variability in spectral data across all sites, Principal Components Analysis (PCA) of the MidIR data was done with Unscrambler 10.3. The spectral data were mean centered before the PCA analysis. The Hotelling's T^2 statistic was used to show the leverage for each sample. An F-test was used to determine its critical limit, and is used to spot spectral outliers.

Sample Selection for the Partial Least Squares Regressions

The Kennard-Stone Sample Selection function of Unscrambler 10.3 was used to select sample subsets for the calibration and validation sample sets. The sample set was split evenly into 248 samples each for the calibration and validation sets. Samples in the calibration set were not part of the validation set. The Kennard-Stone function uses PCA results to uniformly allocate the calibration and validation samples according to the multivariate space in the spectral data (Kennard and Stone, 1969). Separate Kennard-Stone selections were completed for the MidIR and NIR data sets. For the MidIR sample selection, the average (standard deviation) SOC for the calibration set was 16.6 (12.6) g kg^{-1} , and 16.0 (12.1) g kg^{-1} for the validation set. The average (standard deviation) TN for the calibration set was 1.43 (0.92) g kg^{-1} , and 1.41 (0.91) g kg^{-1} for the validation set. The average (standard deviation) POXC for the calibration set was 568.3 (334.4) g kg^{-1} , for the calibration set, and 553.6 (327.3) g kg^{-1} for the validation set. Even though the Kennard-Stone uses variation in the spectral data as the sole criterion to separate the calibration sets, all sites were represented in the calibration and validation sets.

Table 1. Sites included in the study. Values are mean \pm standard error.

| Project name | Location | Description | POXC† | Soil organic carbon | Total N | n | Reference |
|--|------------------------|--|---|---|--|-----|--|
| Watkinsville | Georgia | Cropland and pasture under different management regimes and land-use histories | mg C kg^{-1} soil 813.8 ± 38.79 | g C kg^{-1} soil 18.8 ± 1.1 | g C kg^{-1} soil 1.4 ± 0.1 | 112 | Franzluebbers et al., 2000; Franzluebbers and Stuedemann, 2002 |
| Living Field Laboratory (LFL) | Michigan | Continuous corn vs. Corn-soybean-wheat in 3 managements | 292.3 ± 7.6 | 8.5 ± 0.3 | 2.2 ± 0.4 | 144 | Culman et al., 2013 |
| NY-Grain | New York | Grain farms over gradient of soil fertility | 631.0 ± 11.7 | 18.3 ± 0.4 | 1.7 ± 0.0 | 118 | Schipanski et al., 2010; Schipanski and Drinkwater, 2011 |
| Niles | Kansas | Never-tilled annual crop conversion from tall grass prairie | 464.9 ± 55.1 | 15.5 ± 1.5 | 1.5 ± 0.1 | 36 | Beniston, 2009 |
| Long-Term Research on Agricultural Systems (LTRAS) | Near Davis, California | Long-term systems study with crop rotations and cover crops | 250.2 ± 11.5 | 9.5 ± 0.2 | 1.0 ± 0.0 | 60 | Kong et al., 2005 |
| Ohio Urban Garden (OUG) | Youngstown, Ohio | Urban agriculture experiment with compost, compost+biochar, compost+intensive cover cropping | 803.3 ± 76.4 | 56.0 ± 6.2 | 4.1 ± 0.4 | 24 | Beniston et al., 2015 |
| Kellogg Biological Station (KBS) | Michigan | Long-term experiment; row crops, herbaceous and woody perennials | 783.5 ± 31.0 | 20.2 ± 1.5 | 1.8 ± 0.1 | 56 | Grandy and Robertson, 2007 |

† POXC, permanganate oxidizable carbon.

Partial Least Squares Calibrations

The nonlinear iterative partial least squares PLS method of Unscrambler 10.3 (Camo Software, Oslo, Norway) was used to generate the calibration and validation results (Martens and Naes, 1989). The PLS regression is commonly used to deal with correlated prediction variables (such as infrared spectra), and can be applied when the prediction variables are more numerous than the observations. No spectral outliers were omitted from the calibration models. All NIR and MidIR spectral data were mean centered before the PLS regressions. As explained below, samples from one of the sites were excluded from a subsequent set of calibrations due to a deviation in the SOC to POXC relationship. Separate PLS regressions were performed with detrending, multiplicative scatter correction (MSC), and standard normal variate (SNV) pretreatments of the absorbance data. Detrending involves subtraction of a polynomial or linear fit to reduce baseline artifacts such as tilt, which is sometimes an issue in NIR spectra. The MSC, SNV, and detrending pretreatments were all done in combination with mean centering. The optimal number of factors was determined by the software using the relationship between the explained variances for the calibration and validation sets.

RESULTS

Bands in the MidIR and NIR Spectra by Site

The NIR spectra from the different sites had relatively few features compared to the MidIR region (Fig. 1). Peaks observed in the NIR spectra consist of combinations and overtones from the MidIR, with mixed information about organic material, iron oxides, clays and carbonates (Stenberg et al., 2010). Absorbance

at the higher wavenumbers approaches the visible range and could be indicative of darker soils with iron containing minerals. The main NIR absorbance peaks observed occurred in three spectral ranges: around 7070 cm^{-1} between the first and second overtone region, between 5330 and 4920 cm^{-1} in the first overtone region and combination region, and at 4400 to 4325 cm^{-1} in the combination region.

In the MidIR range, absorption near 3624 to 3620 cm^{-1} , observed as a sharp peak in all sites (Fig. 1b), is due to inner hydroxyl groups in clay lattice sheets (Madejová, 2003). A weak band at 3695 cm^{-1} in most of the sites could be attributed to clay O–H stretching. This band is more pronounced in the Watkinsville soil, which also has sharp peaks at 3455 and 3535 cm^{-1} due to clay O–H stretching. Between 3450 to 3300 cm^{-1} is a broad and slight rise in absorbance due to hydrogen bonded O–H and N–H stretching (Parikh et al., 2014), which has greater O–H influence at the higher range. Between 2925 to 2850 cm^{-1} are the aliphatic C–H anti-symmetric and symmetric stretch bands, observable in most sites except LTRAS, which has low SOM. It has to be noted that absorbance between 2925 to 2850 cm^{-1} can also be due to carbonates (Legodi et al., 2001). The carbonate band at 2520 cm^{-1} (Calderón et al., 2011b), is only observed as a very small rise, especially in the Niles average spectrum. The triplet of silicate peaks between 2000 and 1780 cm^{-1} is due to quartz or kaolinite, as well as sands (Nguyen et al., 1991). All soil spectra contain a peak at 1680 with a shoulder at 1611 cm^{-1} which can be assigned to several moieties including amide C=O stretch (amide I) and quinone or ketone C=O stretch at the higher wavenumbers, and/or aromatic C=C stretch and/or carboxylate C–O asymmetric stretch at the lower wavenumbers (Parikh et al., 2014). The small peak

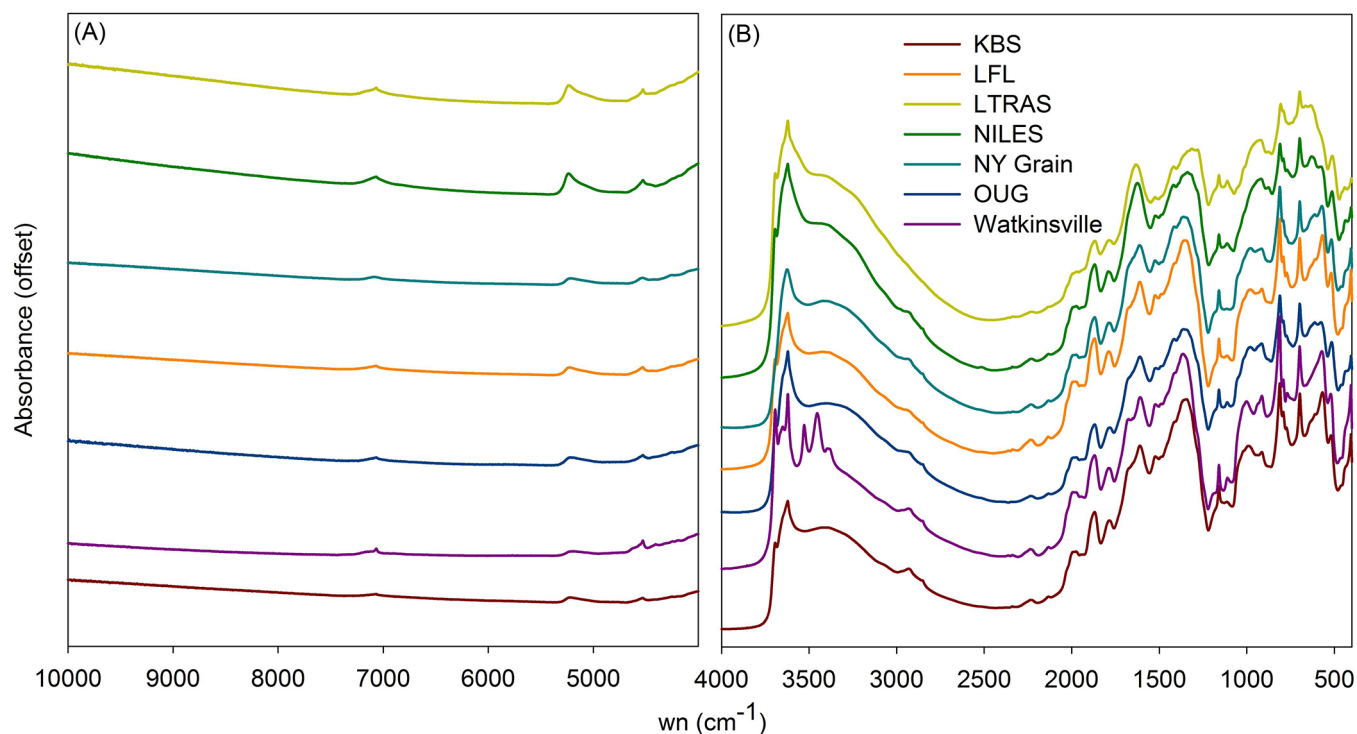


Fig. 1. Diffuse reflectance Fourier transform near-infrared (A) and mid-infrared (B) average spectra for each site. The absorbance was offset to avoid overlap and aid visualization.

at 1520 cm^{-1} is due to the amide II band, and/or aromatic C=C from lignin (Baes and Bloom, 1989). The peak at 1420 cm^{-1} , with the shoulder at 1360 cm^{-1} is due to aliphatic C-H bending (Haberhauer and Gerzabek, 1999). The inverted peaks between 1220 and 1060 cm^{-1} are caused by specular reflection from soil minerals in the neat samples. The peak at 810 cm^{-1} is assigned to amorphous silica.

Correlation of POXC with SOC and TN

Due to the diversity of the sample set, the SOC had a wide range, from 0.8 to 108 g kg^{-1} (Fig. 2). Likewise the TN ranged from 0.3 to 7.9 g kg^{-1} . The POXC had maxima around 1400 mg C kg^{-1} . The best fit between SOC and POXC was hyperbolic rather than linear ($R^2 = 0.71$), given that SOC values higher than $\sim 50\text{ g kg}^{-1}$ were not associated with further increases in POXC values. The OUG samples are responsible for the marked deviation from the regression line among the high SOC soil samples (Fig. 2). Without OUG samples, the best fit relationship is linear ($R^2 = 0.99$). This indicates that the POXC values for OUG fall below the best fit line not due to POXC saturation but rather to the different quality of the soil C caused by the history

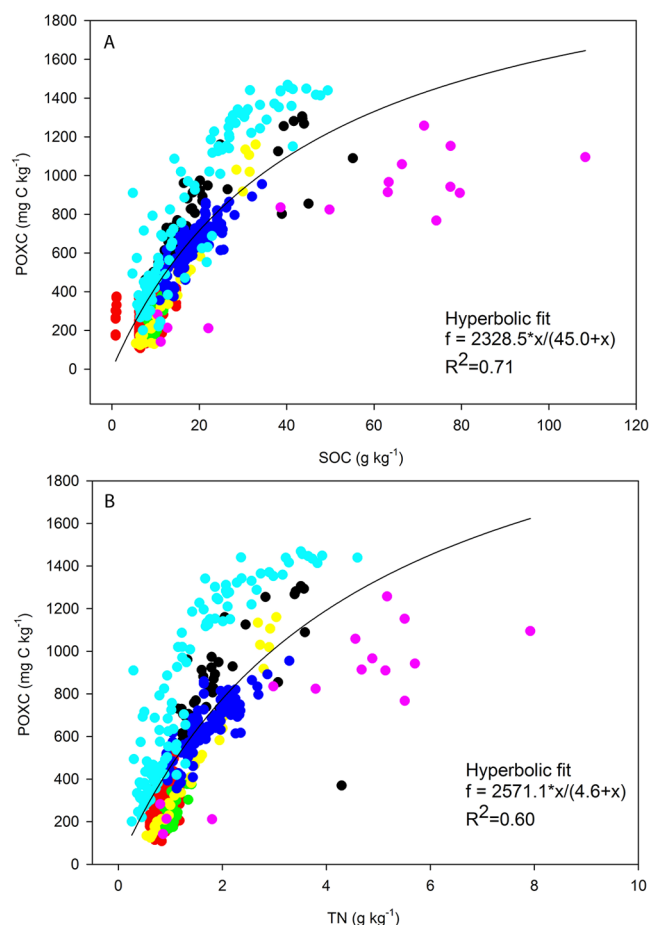


Fig. 2. Hyperbolic fit lines for the soil organic carbon (SOC) vs. permanganate oxidizable carbon (POXC) (A), and soil total nitrogen (TN) vs. POXC (B). Kellogg Biological Station samples are in black, Living Field Laboratory samples are in red, Long-Term Research on Agricultural Systems samples are in green, Niles samples are in yellow, NY-Grain samples are in blue, Watkinsville samples are in light blue, and Ohio Urban Garden samples are in pink.

of amendments that may not have entered the slightly more processed POXC pool. The TN and POXC had very similar correlation pattern to that of SOC and POXC, given that SOC and TN were themselves highly linearly correlated ($R^2 = 0.95$).

Spectral Diversity

Ideally, the spectra for a calibration set should form a cohesive set to avoid calibration performance artifacts caused by bimodal distributions. The spectra from the different sites all formed a single cloud in multivariate space, although scores along PC1 and PC2 do show separations between individual sites within that cloud (Fig. 3a). Samples from KBS and some samples from Watkinsville had low Component 1 scores, and loadings indicate that this was due to low clay (3620 cm^{-1}) and clay/amide-like absorbance (1649 cm^{-1} ; Fig. 3b). Component 2 clearly separated LFL from Niles and LTRAS due to differences in texture as shown by loadings from clay and Si-O bands. Component 2 also separates KBS from Niles and LTRAS. A few MidIR spectral outliers in the LFL and LTRAS sets were detected according to the Hotelling T^2 statistic. However, these samples were not excluded from the PLS regressions as there was no specific reason to suspect that their C pool data were faulty, and because of our aim to ascertain the value of infrared-based

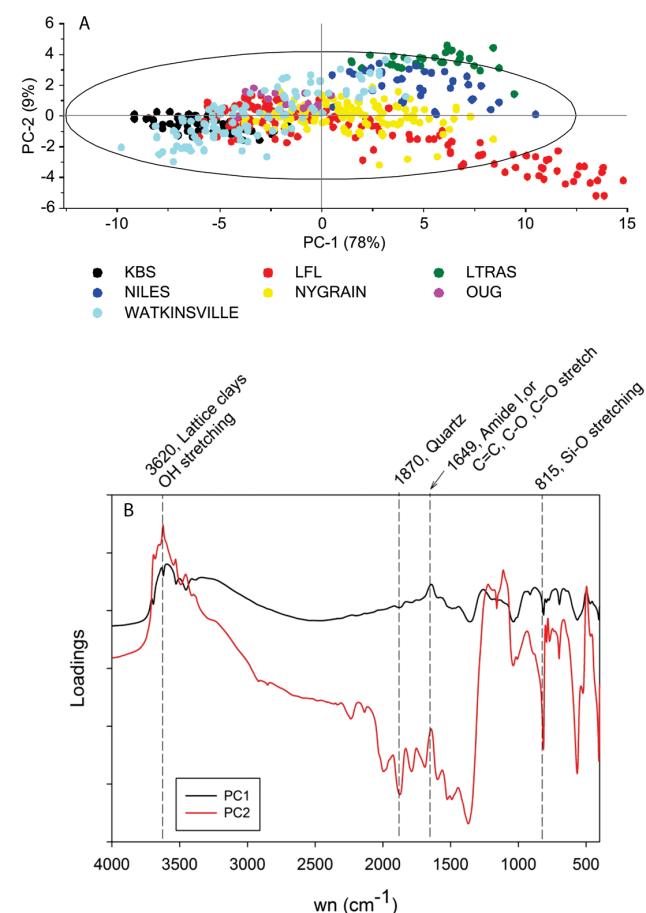


Fig. 3. Principal components analysis of the mid-infrared spectra data of all the sites. Scores (A), and component 1 and 2 loadings (B). The variation explained by each component is shown in parenthesis. The Hotelling T^2 ellipse in Panel A shows the spectral outliers.

calibrations for POXC in a wide geographic scale. The OUG samples, which had an anomalous relationship between POXC and SOC (Fig. 2), were not spectral outliers (Fig. 3).

MidIR and NIR Partial Least Squares Calibrations for POXC

The MidIR and NIR spectral data were used to generate predictive PLS models for POXC (Fig. 4). The MidIR spectra produced calibrations for POXC, with R^2 that varied from 0.78 to 0.81 depending on the mathematical pretreatment of the absorbance data (Table 2). The validation R^2 were similar to the calibration R^2 . The SNV, detrending, and MSC pretreatments all gave small improvements in R^2 and RMSE over the mean centering alone with SNV but detrending was slightly better. Calibrations performed with the NIR attained R^2 of 0.73 to 0.88, but the validation R^2 were lower, ranging from 0.66 to 0.76. As with the MidIR, the detrended pretreatment of the NIR spectra gave best calibration and validation results compared to the rest of the pretreatments. Figure 5 shows the degradation of the validation quality after eight PLS factors with the NIR. Calibrations for SOC and TN had R^2 and RMSE of lower quality than those for the POXC regardless of the spectral range used, with calibration R^2 always below 0.59 for all three spectral pretreatments.

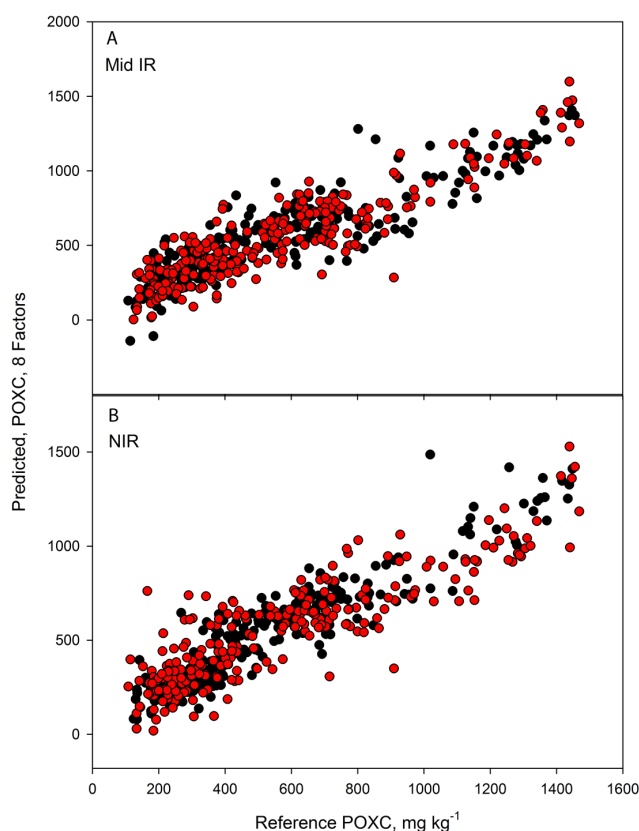


Fig. 4. Partial least squares regression predicted permanganate oxidizable carbon (POXC) vs. reference POXC values for the calibration (black dots) and the validation (red dots) for the mid-infrared and near-infrared data. The spectral data were pre-treated with detrending for both the mid-infrared range (A) and the near-infrared range (B).

Correlation of POXC with MidIR and NIR Spectral Bands

A correlation analysis between the MidIR absorbance and the POXC, SOC, and TN data shows that the three analytes were positively correlated with absorbance at 2930 to 2850 cm^{-1} ($R > 0.38$), attributed to aliphatic C–H stretch (Fig. 6a). The correlation with POXC and the peak at 2920 cm^{-1} was slightly stronger ($R^2 = 0.43$) than the correlation with SOC ($R^2 = 0.39$). In contrast, the POXC, SOC, and TN were all negatively correlated to quartz absorbance between ~ 2050 and 1835 cm^{-1} . Permanganate oxidizable C has a higher R^2 than SOC and TN for the region between 2730 and 2530 cm^{-1} , a region assigned to carboxylic acid H-bonded O–H (Parikh et al., 2014). Conversely, POXC has a negative correlation coefficient for the 3380 to 3100 cm^{-1} region assigned to O–H, N–H and at lower range to aromatic C–H stretch.

The correlation patterns with the NIR data were similar for POXC, SOC, and TN. The highest R scores were achieved between 4875 and 4650 cm^{-1} , whereas the lowest R scores occurred between 5350 and 5180 cm^{-1} (Fig. 6b). The POXC had the highest absolute values for the R scores in these two NIR spectral regions. While it is not straightforward to assign specific chemistries to absorbances within the NIR, soil absorbance bands between 2050 and 2150 nm (4875–4650 cm^{-1}) have been assigned to $4\nu_1$ overtones of polysaccharide C–O, and to overtones of amine N–H (Viscarra Rossel and Behrens, 2010).

Partial Least Squares using Selected MidIR Spectral Region

Besides the calibrations utilizing the full MidIR spectral range, calibrations were also calculated using a selected spectral region determined by the R coefficient between the MidIR spectral data and POXC. The region between 3225 and 2270 cm^{-1} encompasses absorbance for aliphatic C–H and O–H plus N–H, and contains spectral bands that are the most positively correlated with the POXC (Fig. 6). This region is mainly organic, and has little mineral interference in soils that are low in carbonates, such as those in the data set (Reeves, 2012). The selected region contains 27% of the data in the full MidIR range, with a total of 496 spectral data points. In both the SOC and TN cases the calibration quality deteriorated by using the selected region rather than the full MidIR spectrum. The SOC prediction with the selected region had R^2 of 0.48 and 0.60 for the calibration and validation, with RMSE of 9.0 and 7.6. The TN prediction attained R^2 of 0.46 and 0.55 for the calibration and validation, with RMSE of 0.67 and 0.61. The POXC prediction with the selected region, however, had a slight deterioration in quality compared to the PLS using the full MidIR spectrum, with an R^2 of 0.76 and 0.77 for the calibration and validation, and RMSE of 162.0 and 154.0 (Fig. 7). It should be noted that a correlation of the single absorbance at 2920 cm^{-1} and the POXC data had a R^2 of 0.43, showing that a single point calibration is not sufficient for predicting POXC.

Site Effects on Calibration Quality

The predictive ability of the calibrations varied widely between sites (Table 3). Calibrations based on the full MidIR spectrum had the best predictions for the LTRAS and Niles samples, while the OUG had the largest RMSE, regardless of whether the full spectrum or selected region was used for the PLS regression. The POXC prediction for KBS, LFL, and Niles deteriorated with the selected MidIR region relative to the full spectrum. As with the MidIR, the PLS regression based on the NIR also had the LTRAS site with the lowest RMSE of the prediction, and OUG with the poorest predictions for the three analytes. The NIR-based predictions for TN and SOC followed similar patterns to those of the POXC, with the OUG site samples having the poorest calibration results.

The unusual relationship between POXC and SOC observed in the OUG samples (Fig. 2) prompted us to carry out additional PLS calibrations leaving out the OUG samples (Table 4). A comparison of the PLS calibrations including all sites (Table 2) with the PLS calibrations without the OUG sites (Table 4) shows that predictions for POXC were not markedly affected by the removal of the OUG samples from the set. However, predictions for SOC and TN were markedly better when the OUG samples were excluded, as indicated by increased R^2 and decreased RMSE.

DISCUSSION

Our results show that both the MidIR and NIR data can be used to determine POXC on a wide range of soils. Calibrations for TN and SOC were not as good as they were for POXC when the full sample set was used. However, calibration quality improved markedly when the OUG samples were removed. Therefore, this work shows that anomalous soils in the sample set have to be identified and taken into account to properly predict soil C pools with infrared spectral data. Selected spectral regions could be used instead of the full MidIR spectrum in calibrations for POXC, albeit a slightly increased RMSE.

Others have found that, depending on the soil, SOC can sometimes be positively correlated with POXC (Lucas and Weil, 2012; Culman et al., 2012; Veum et al., 2014). Veum et al. (2014) showed that POXC correlates positively with other measures of soil quality such as enzyme activities and aggregation in a soil from the North American Corn Belt. In this study, with a more geographically diverse sample set, POXC had a hyperbolic correlation to SOC and TN. There was a point after $\sim 50 \text{ g kg}^{-1}$ of POXC content where POXC declined with increasing SOC. This hyperbolic relationship is largely a result

Table 2. Spectral pretreatment effects on partial least squares calibration quality using mid-infrared (MidIR) and near-infrared (NIR) spectral data. Calibration (Cal) and validation (Val) sets consisted of different samples selected using the Kennard-Stone function. Permanganate oxidizable C units are mg C kg^{-1} soil, SOC and TN units are g C kg^{-1} soil. Note that the standard normal variate (SNV), detrending (Detrend), and multiplicative scatter correction (MSC) were all applied together with mean centering.

| | | POXC | | SOC | | TN | |
|-------------|---------|--------------------|-------------------|-----------------|-------------------|-----------------|-------------------|
| | Factors | R^2 (Cal/Val) | RMSE (Cal/Val) | R^2 (Cal/Val) | RMSE (Cal/Val) | R^2 (Cal/Val) | RMSE (Cal/Val) |
| MidIR | | | | | | | |
| Mean center | 6 | 0.78/0.77 | 157.1/156.0 | 0.44/0.55 | 9.4/8.0 | 0.45/0.55 | 0.68/0.61 |
| SNV | 9 | 0.81/0.81 | 144.3/144.3 | 0.54/0.70 | 8.5/6.7 | 0.54/0.66 | 0.62/0.53 |
| Detrend | 8 | 0.81/0.81 | 145.8/143.8 | 0.52/0.64 | 8.6/7.2 | 0.52/0.63 | 0.63/0.55 |
| MSC | 9 | 0.81/0.80 | 145.1/146.6 | 0.55/0.69 | 8.5/6.8 | 0.54/0.65 | 0.62/0.53 |
| NIR | | | | | | | |
| Mean center | 9 | 0.83/0.75 | 126.6/174.9 | 0.58/0.52 | 7.5/9.1 | 0.56/0.51 | 0.57/0.67 |
| SNV | 7 | 0.83/0.71 | 130.0/188.5 | 0.56/0.47 | 7.7/9.5 | 0.54/0.47 | 0.59/0.70 |
| Detrend | 8 | 0.88/0.76 | 110.1/169.5 | 0.59/0.50 | 7.4/9.2 | 0.58/0.51 | 0.56/0.67 |
| MSC | 5 | 0.73/0.66 | 161.7/201.4 | 0.49/0.40 | 8.3/10.1 | 0.43/0.37 | 0.65/0.76 |

of the OUG samples not conforming to the best fit line, and to some extent a methodological artifact with the upper detection limit of POXC. The methodological artifact occurs when calculating POXC with the assumptions laid out by Weil et al. (2003). Using 2.5 g of soil, $1440 \text{ mg POXC kg soil}^{-1}$ is the maximum amount detectable in a sample as 100% of the permanganate is oxidized at 1440 mg POXC . Increasing the detection limits would require method manipulation beyond the scope of this

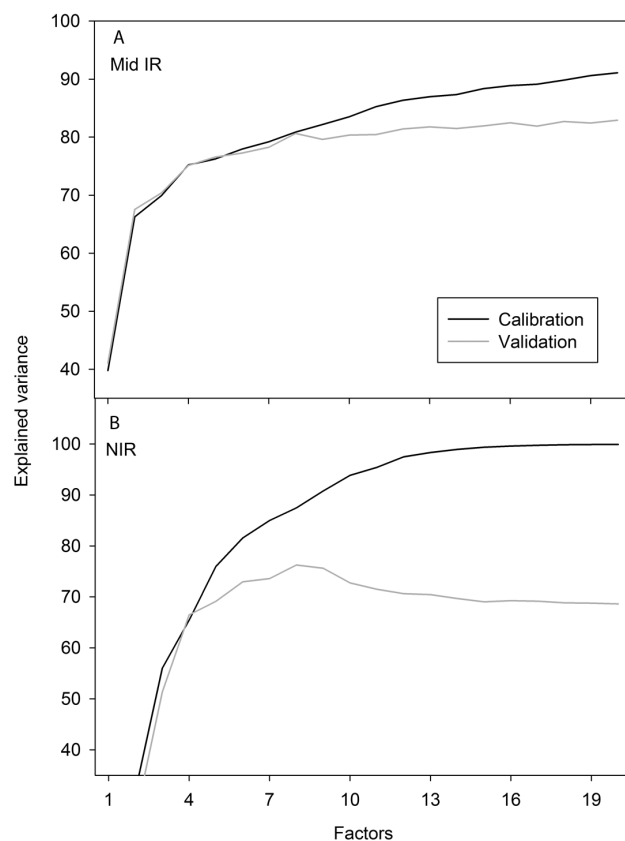


Fig. 5. Explained variances for the near-infrared and mid-infrared partial least squares regressions. The spectral data were pre-treated with detrending for both the mid-infrared range (A) and the near-infrared range (B).

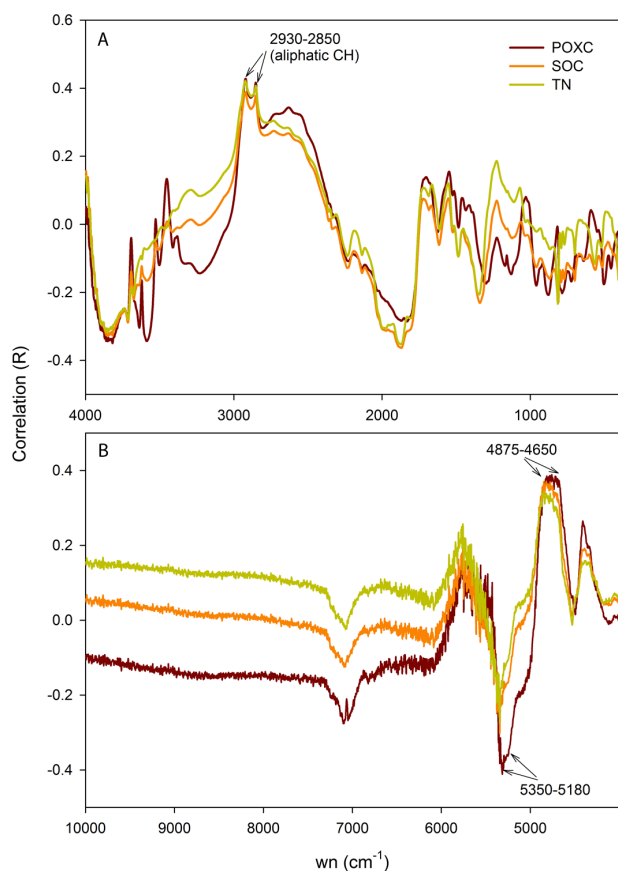


Fig. 6. Correlation coefficients of specific spectral bands with soil organic carbon (SOC), permanganate oxidizable carbon (POXC) and total soil nitrogen (TN) for the mid-infrared range (A) and the near-infrared range (B).

study, such as increasing the concentration of permanganate or decreasing the amount of soil reacted. Deviations from the conventional POXC method would also make it impossible to compare our results to those of others.

The main reason for the hyperbolic fit in our sample set was due to the anomalous OUG samples, given that the relationship

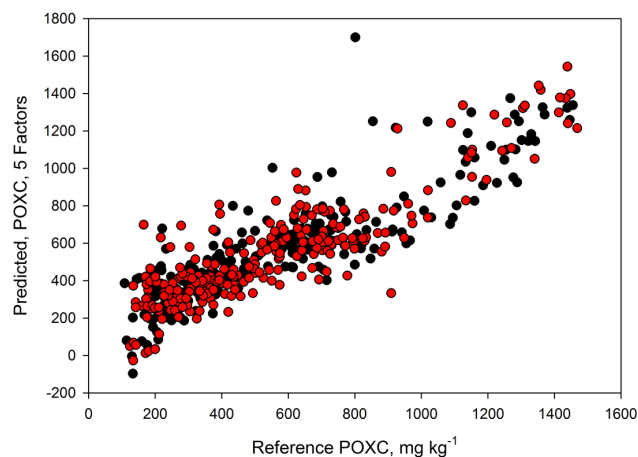


Fig. 7. Partial least squares (PLS) regression predicted permanganate oxidizable carbon (POXC) vs. reference POXC values for the calibration (black dots) and the validation (red dots) for a selected region of the mid-infrared data. Only the region between 3225 and 2270 cm⁻¹ was used for the PLS regression.

is linear without the OUG in the regression. The nonlinear relationship below the upper limit occurs because OUG received organic amendments that altered the relationship between labile and total soil C. The OUG also have higher light fraction POM, which is not well correlated with POXC (Culman et al., 2012). The hyperbolic relationship may also be indicating that in general, soils high in SOC tend to have proportionally less labile C than soils with lower SOM. However, this would be difficult to argue, given the previous consideration that maximum detection of POXC was already achieved. While the relationship between different C pools is still an active area of study, previous work comparing asymptotic vs. linear C saturation fit has indicated that relatively labile soil C can approach a maximum level as SOC increases (Six et al., 2002).

Previous work has shown that MidIR bands in diffuse reflectance spectra can offer a semi-quantitative estimate of organic moieties and minerals (Calderón et al., 2013). Diffuse reflectance spectra do not fully conform to Beer-Lambert law due to the uncertain path length and low penetration of the MidIR energy (Calderón et al., 2013; Margenot et al., 2015). Nevertheless, increases in absorbance bands can lead to useful hypothesis generation and also to assessment of management effects on SOC of soils with similar mineral backgrounds (Calderón et al., 2011a). There was high spectral diversity between the sites included in this study, although no single site formed a separate cluster from the whole set as illustrated with the PCA. The main spectral differences accounting for most of the variation between the sites are due to mineral bands. Minerals make up a larger portion of the soil's mass than the organic materials, and it is thus expected that soils of different age and parent material have different MidIR absorbance patterns. The spectra associated with Watkinsville and KBS have particularly high absorbance for the lattice clay band at 3620 cm⁻¹, as well as at 1649 cm⁻¹, which is often assigned to amides but is also present in clay spectra (Madejová, 2003). The Watkinsville and KBS samples also have MidIR bands consistent with higher sand content, with high absorbance at 1790 to 2000 cm⁻¹ and at the specular reflection inversion between 1220 and 1060 cm⁻¹. The LFL also has distinct clay and Si–O signals relative to Niles and LTRAS. Given that excluding the mineral bands from the calibration set did not drastically decrease the calibration performance, we can conclude that mineral absorbances do not contribute to chemometric analysis of labile C.

This study shows that PLS calibrations based on NIR and MidIR spectral data can be used to generate useable calibrations for POXC, with $R^2 < 0.8$, and the predictions were slightly better for MidIR compared to NIR as shown by the validation coefficient of determination. The RMSE is a measure of the dispersion of the calibration or validation samples around the regression line, and it showed the differences between POXC values and the predictions using absorbance data in the same units as those of the variable in question. The minimal advantage of the MidIR over the NIR in terms of the POXC calibration quality is reflected on the mixed RMSE results.

Absorbance data pretreatments are sometimes useful during calibration development because spectral variation that is not associated to soil composition is minimized. Artifact spectral variations can be due to particle size variations, changes in refractive index, sample packing variability, and/or surface irregularities (Reeves et al., 2012). These factors can affect the effective path length of the infrared radiation, and cause additive or multiplicative wavelength-dependent artifacts like baseline shifts, tilt or curvature variation. Different pretreatments can improve the accuracy of the prediction for specific spectral regions and particular sample properties (Calderón et al., 2007, 2009). However, this is not always the case. In a study to predict soil total N, it was shown that several different pretreatment methods did not improve PLS calibrations (Fang et al., 2015). Particle size artifacts could have potentially been a problem in a highly diverse sample set such as ours. In this study, detrending plus mean centering pretreatment resulted in very minor improvements in the calibrations for both the NIR and MidIR compared to mean centering alone. The small magnitude of the benefits attained with the pretreatments suggests that textural artifacts were not important in our analysis.

MidIR and NIR data have been used to successfully predict many soil attributes besides total C, such as aromaticity, microbial biomass, mineralizable C, and aggregate C (Reeves et al., 2006, 2012; Thomsen et al., 2009). Infrared absorbance data have generated accurate predictions of labile SOC (Chang et al., 2001; Thomsen et al., 2009). Soriano-Disla et al. (2014) found that both MidIR and NIR predicted soil C, TN, soil water content, texture, CEC, exchangeable calcium and magnesium, pH, metal concentration, as well as microbial biomass and activity. However, MidIR produced better predictions than NIR in general, but NIR outperformed MidIR for several biological properties like enzyme activities and N mineralization. Veum et al. (2014) showed that NIR tends to outperform MidIR in the prediction of POXC. However, their study was based on a localized soil type under a variety of agronomic management regimes, so these results might not apply to soils from other regions. Further, they used spectra from soils demineralized with hydrofluoric acid instead of whole soil spectra, thus their results cannot be compared to our study.

In this study, the predictions for POXC were overall much better than the predictions for TN and SOC when all the sites were included in the PLS model. Better calibrations for POXC could have been explained by a larger coefficient of variation of the POXC data compared to SOC and TN, except that this was not the case with our data set. Alternatively, it is

Table 3. Predicted vs. reference root mean squared errors for the partial least squares (PLS) regressions of the calibration set (Cal) and validation set (Val). Analytes predicted are permanganate oxidizable C (POXC), soil organic C (SOC), and soil total N (TN). The PLS for the near-infrared (NIR) and mid-infrared (MidIR) full spectrum used 8 factors and had mean centering and detrending pretreatments. The PLS using the selected MidIR region (3225–2270 cm^{-1}) used 5 factors and had a mean centering pretreatment. Permanganate oxidizable C units are mg C kg^{-1} soil. SOC and TN units are g C kg^{-1} soil.

| Site† | MidIR full spectrum | | MidIR selected region | | NIR full spectrum | |
|--------------|---------------------|-------|-----------------------|-------|-------------------|-------|
| | Cal | Val | Cal | Val | Cal | Val |
| POXC | | | | | | |
| All | 145.8 | 143.8 | 162.0 | 154.0 | 110.1 | 169.5 |
| KBS | 174.7 | 131.9 | 248.5 | 165.1 | 100.5 | 198.5 |
| LFL | 109.3 | 118.3 | 121.7 | 153.0 | 66.6 | 131.7 |
| LTRAS | 60.7 | 90.9 | 60.3 | 80.2 | 55.2 | 73.3 |
| Niles | 84.4 | 95.2 | 144.8 | 131.4 | 143.4 | 173.9 |
| NY-Grain | 166.0 | 155.5 | 144.5 | 156.1 | 107.1 | 140.4 |
| OUG | 246.7 | 150.7 | 249.8 | 119.1 | 181.0 | 251.7 |
| Watkinsville | 160.9 | 188.7 | 177.6 | 175.2 | 143.7 | 224.5 |
| SOC | | | | | | |
| All | 8.6 | 7.2 | 9.1 | 7.6 | 7.4 | 9.2 |
| KBS | 5.0 | 5.6 | 6.0 | 5.1 | 7.6 | 8.1 |
| LFL | 4.5 | 3.6 | 4.6 | 4.6 | 4.1 | 4.7 |
| LTRAS | 2.4 | 3.2 | 3.3 | 3.3 | 1.9 | 2.9 |
| Niles | 2.7 | 2.9 | 4.4 | 4.0 | 5.2 | 2.6 |
| NY-Grain | 7.4 | 7.1 | 5.5 | 6.4 | 4.9 | 4.5 |
| OUG | 41.3 | 27.0 | 46.4 | 30.2 | 36.7 | 41.9 |
| Watkinsville | 4.6 | 4.9 | 3.3 | 4.0 | 3.2 | 4.0 |
| TN | | | | | | |
| All | 0.63 | 0.55 | 0.67 | 0.61 | 0.56 | 0.67 |
| KBS | 0.37 | 0.68 | 0.49 | 0.72 | 0.66 | 0.56 |
| LFL | 0.31 | 0.25 | 0.29 | 0.33 | 0.25 | 0.32 |
| LTRAS | 0.16 | 0.20 | 0.23 | 0.26 | 0.16 | 0.24 |
| Niles | 0.34 | 0.33 | 0.34 | 0.27 | 0.31 | 0.30 |
| NY-Grain | 0.57 | 0.56 | 0.52 | 0.59 | 0.48 | 0.40 |
| OUG | 2.87 | 1.70 | 3.22 | 1.89 | 2.37 | 2.85 |
| Watkinsville | 0.40 | 0.45 | 0.38 | 0.46 | 0.42 | 0.50 |

† KBS, Kellogg Biological Station; LFL, Living Field Laboratory; LTRAS, Long-Term Research on Agricultural Systems; OUG, Ohio Urban Garden.

possible that the higher R^2 for POXC can be explained by the higher correlation coefficients of the spectral data to POXC than to SOC. This was especially true for the NIR, where the

Table 4. Partial least squares regression calibration quality using mid-infrared (MidIR) and near-infrared (NIR) spectral data. Samples from the Ohio Urban Garden site were left out of the model. Calibration (Cal) and validation (Val) sets consisted of different samples selected using the Kennard-Stone function. Permanganate oxidizable C (POXC) units are mg C kg^{-1} soil, SOC and TN units are g C kg^{-1} soil. Note that the detrending pretreatment was applied together with mean centering. The calibration and validation sets had 238 samples each.

| | | POXC | | SOC | | TN | |
|--------------|---|--------------------|-------------------|--------------------|-------------------|--------------------|-------------------|
| | | R^2 (Cal/Val) | RMSE (Cal/Val) | R^2 (Cal/Val) | RMSE (Cal/Val) | R^2 (Cal/Val) | RMSE (Cal/Val) |
| MidIR | | | | | | | |
| Mean center | 7 | 0.81/0.78 | 143.4/149.1 | 0.80/0.77 | 4.1/4.2 | 0.68/0.74 | 0.42/0.35 |
| Detrending | 6 | 0.79/0.78 | 151.2/149.6 | 0.69/0.78 | 4.3/4.2 | 0.66/0.73 | 0.43/0.36 |
| NIR | | | | | | | |
| Mean center | 7 | 0.75/0.76 | 164.5/159.2 | 0.68/0.70 | 5.2/4.9 | 0.69/0.56 | 0.38/0.49 |
| Detrending | 6 | 0.84/0.80 | 133.7/146.5 | 0.74/0.69 | 4.7/4.9 | 0.71/0.57 | 0.37/0.49 |

absorbance at 5350–5180 cm^{-1} and at 4875 to 4650 cm^{-1} were better correlated to POXC than to SOC. In the MidIR, carboxylic acid H-bonded O–H absorbances at 3380 to 3100 cm^{-1} , as well as bands at 2930 to 2850 cm^{-1} were more correlated to POXC content than to SOC content. Previous work has shown that the asymmetric and symmetric stretching of C–H in CH_2 at 2930 and 2850 cm^{-1} is related to the decomposition state of soils, and has been used in band ratio analysis to study labile soil C (Veum et al., 2014), and could serve as an indicator of SOC lability in some soils (Demyan et al., 2012). The aliphatic C–H MidIR band correlates with total aliphatic C–H as measured by NMR (Veum et al., 2014), but the presence of carbonates in the soil sample can complicate this assignment in calcareous soils (Legodi et al., 2001). Because of this, future studies should evaluate the relationship between absorbance at 2930 to 2850 cm^{-1} and POXC in highly calcareous soils.

The MidIR spectrum, when collected at the range and resolution used in this study, contains more than 1800 data points. This prompts the question of whether some of the spectral information is in effect noise that could be omitted from the calibration. For this reason, we explored the possibility of using a reduced range of spectral data, informing the selection with a correlation analysis between the POXC and the absorbance data. A previous study showed that POXC correlates with the aliphatic C–H spectral bands in soils from the Central Valley of California under organic vegetable production (Margeot et al., 2015). The results from our study on soils from a wide geographic area and under different agricultural managements further corroborate the finds that POXC was related to aliphatic C–H compounds. Restricting the spectral range used in the chemometric analysis to the aliphatic C–H region and adjacent bands, did not markedly reduce the calibration quality for POXC. The region selection approach showed potential given that the resulting calibration could be considered useful if a R^2 of 0.77 is acceptable.

A fundamental issue affecting chemometric prediction of soil attributes is how many different types of soils can be predicted with a single calibration (Viscarra Rossel and Behrens, 2010). In this study, we showed that removing the OUG samples from the calibration set markedly improved the prediction of SOC, but not POXC. Several studies have examined the use of localized versus large-scale calibrations (Cobo et al., 2010; Guerrero et al., 2010; Minasny et al., 2009; Reeves and Smith, 2009; Wetterlind et al., 2010). However, there is no consensus about the precise basis on which decisions about calibration sets should be made. In this study it is apparent that the OUG samples should require a separate calibration for SOC, while they could be included with the rest of the sites when calibrating for POXC. The OUG site was not a spectral outlier, but had a relatively low number of samples, and high standard error for the POXC and SOC. The different biochar and compost amendments likely added inordinate amounts of non-resident and stable SOC. Besides, the OUG project was based on a highly diverse set of urban soils with high levels of spatial heterogeneity (Beniston and Lal, 2012). We hypothesize that the addition of

compost might have altered the chemistry of the SOC enough that the relationship between POXC and the molecular makeup of the SOC was altered and the calibration was not able to properly predict POXC in those particular samples.

CONCLUSIONS

The PLS calibrations for POXC using NIR data gave acceptable results, whereas calibrations using MidIR were of slightly better quality. Selecting specific regions within the MidIR gave comparable calibrations to those using the whole spectrum. Aliphatic C–H and carboxylic acid H-bonded OH bands were highly correlated to POXC, suggesting that they should be considered of particular importance for the study of labile soil C, and can be used in a reduced spectral data set to predict POXC. The chemometric quantitation for SOC benefitted from the exclusion of samples from an urban site in which a variety of organic amendments had been deployed, affecting the relationship between SOC and POXC. Our results have broader implications for the study of SOC and soil quality given that a rapid and accurate method for quantifying labile soil C is needed. Further studies should examine the feasibility of using new generation handheld spectrometers for the determination of soil quality parameters in the field.

ACKNOWLEDGMENTS

The authors would like to thank Sieglinde Snapp, Rattan Lal, Laurie Drinkwater, G. Phil Robertson and Jerry Glover for their contribution to this research.

REFERENCES

- Baes, A.U., and P.R. Bloom. 1989. Diffuse reflectance and transmission Fourier transform infrared (DRIFT) spectroscopy of humic and fulvic acids. *Soil Sci. Soc. Am. J.* 53:695–700. doi:10.2136/sssaj1989.03615995005300030008x
- Bellon-Maurel, V., and A. McBratney. 2011. Near-infrared (NIR) and mid-infrared (MIR) spectroscopic techniques for assessing the amount of carbon stock in soils- Critical review and research perspectives. *Soil Biol. Biochem.* 43:1398–1410.
- Beniston, J. 2009. Soil organic carbon dynamics and tallgrass prairie land management. M.S. Thesis. Ohio State Univ., Columbus, OH.
- Beniston, J., and R. Lal. 2012. Improving soil quality for urban agriculture in the North Central U.S. In: R. Lal and B. Augustin, editors, *Carbon sequestration in urban ecosystems*. Springer, Dordrecht, the Netherlands. p. 279–313. doi:10.1007/978-94-007-2366-5_15
- Beniston, J.W., R. Lal, and K. Mercer. 2015. Assessing and managing soil quality for urban agriculture in a degraded vacant lot soil. *Land Degrad. Dev.* 27(4). doi:10.1002/ldr.2342
- Calderón, F., M. Haddix, R. Conant, K. Magrini-Bair, and E.A. Paul. 2013. Diffuse-reflectance Fourier-transform mid-infrared spectroscopy as a method of characterizing changes in soil organic matter. *Soil Sci. Soc. Am. J.* 77:1591–1600. doi:10.2136/sssaj2013.04.0131
- Calderón, F.J., M.M. Mikha, M.F. Vigil, D.C. Nielsen, J.G. Benjamin, and J.B. Reeves. 2011a. Diffuse-reflectance mid-infrared spectral properties of soils under alternative crop rotations in a semi-arid climate. *Commun. Soil Sci. Plant Anal.* 42:2143–2159. doi:10.1080/00103624.2011.596243
- Calderón, F.J., J.B. Reeves, H.P. Collins, and E.A. Paul. 2011b. Chemical differences in soil organic matter fractions determined by diffuse-reflectance mid-infrared spectroscopy. *Soil Sci. Soc. Am. J.* 75:568–579. doi:10.2136/sssaj2009.0375
- Calderón, F.J., J.B. Reeves, J.G. Foster, W.M. Clapham, J.M. Fedders, M.F. Vigil, and W.B. Henry. 2007. Comparison of diffuse reflectance Fourier transform mid-infrared and near-infrared spectroscopy with grating-based near-infrared for the determination of fatty acids in forages. *J. Agric. Food*

- Calderón, F.J., M.F. Vigil, J.B. Reeves, and D.J. Poss. 2009. Mid-infrared and near-infrared calibrations for nutritional parameters of triticale (*Triticosecale*) and pea (*Pisum sativum*). J. Agric. Food Chem. 57:5136–5142. doi:10.1021/jf803936x
- Chang, C., D.A. Laird, M.J. Mausbach, and J.C.R. Hurburgh. 2001. Near-infrared reflectance spectroscopy-Principal components regression analyses of soil properties. Soil Sci. Soc. Am. J. 65:480–490. doi:10.2136/sssaj2001.652480x
- Cobo, J.G., G. Dercon, T. Yekeye, L. Chapungu, C. Kadzere, A. Murwira, R. Delve, and G. Cadisch. 2010. Integration of mid-infrared spectroscopy and geostatistics in the assessment of soil spatial variability at landscape level. Geoderma 158:98–411. doi:10.1016/j.geoderma.2010.06.013
- Culman, S.W., S.S. Snapp, M.A. Freeman, M.E. Schipanski, J. Beniston, R. Lal, L.E. Drinkwater, A.J. Franzluebbers, J.D. Glover, S.A. Grandy, J. Six, J.E. Maul, S.E. Mirsky, J.T. Spargo, and M.M. Wander. 2012. Permanganate oxidizable carbon reflects a processed soil fraction that is sensitive to management. Soil Sci. Soc. Am. J. 76:494–504. doi:10.2136/sssaj2011.0286
- Culman, S.W., S.S. Snapp, J.M. Green, and L.E. Gentry. 2013. Short- and Long-Term labile soil carbon and nitrogen dynamics reflect management and predict corn agronomic performance. Agron. J. 105: 493–502.
- de Moraes Sá, J.C., F. Tivet, R. Lal, C. Briedis, D.C. Hartman, J.Z. dos Santos, and J.B. dos Santos. 2014. Long-term tillage systems impacts on soil C dynamics, soil resilience and agronomic productivity of a Brazilian Oxisol. Soil Tillage Res. 136:38–50. doi:10.1016/j.still.2013.09.010
- Demyan, M.S., F. Rasche, E. Schulz, M. Breulmann, T. Muller, and G. Cadisch. 2012. Use of specific peaks obtained by diffuse reflectance Fourier transform mid-infrared spectroscopy to study the composition of organic matter in a Haplic Chernozem. Eur. J. Soil Sci. 63:189–199. doi:10.1111/j.1365-2389.2011.01420.x
- Fang, X.-R., H.-L. Zhang, L.-X. Huang, and Y. He. 2015. Measurement of soil total nitrogen using near infrared spectroscopy combined with RCA and SPA. Guangpuxue Yu Guangpu Fenxi 35:1248–1252.
- Franzluebbers, A.J., and J.A. Stuedemann. 2002. Particulate and non-particulate fractions of soil organic carbon under pastures in the Southern Piedmont USA. Environ. Poll. 116:S53–S62. doi:10.1016/S0269-7491(01)00247-0
- Franzluebbers, A.J., J.A. Stuedemann, H.H. Schomberg, and S.R. Wilkinson. 2000. Soil organic C and N pools under long-term pasture management in the Southern Piedmont USA. Soil Biol. Biochem. 32:469–478. doi:10.1016/S0038-0717(99)00176-5
- Grandy, A.S., and G.P. Robertson. 2007. Land-use intensity effects on soil organic carbon accumulation rates and mechanisms. Ecosystems 10:58–73. doi:10.1007/s10021-006-9010-y
- Guerrero, C., R. Zornoza, I. Gomez, and J. Mataix-Beneyto. 2010. Spiking of NIR regional models using samples from target sites: Effect of model size on prediction accuracy. Geoderma 158:66–77. doi:10.1016/j.geoderma.2009.12.021
- Haberhauer, G., and M.H. Gerzabek. 1999. Drift and transmission FT-IR spectroscopy of forest soils: An approach to determine decomposition processes of forest litter. Vib. Spectrosc. 19:413–417. doi:10.1016/S0924-2031(98)00046-0
- Kennard, R.W., and L.A. Stone. 1969. Computer aided design of experiments. Technometrics 11:137–148. doi:10.1080/00401706.1969.10490666
- Kong, A.Y.Y., J. Six, D.C. Bryant, R.F. Denison, and C. van Kessel. 2005. The relationship between carbon input, aggregation, and soil organic carbon stabilization in sustainable cropping systems. Soil Sci. Soc. Amer. J. 69:1078–1085. doi:10.2136/sssaj2004.0215
- Legodi, M.A., D. de Waal, J.H. Potgieter, and S.S. Potgieter. 2001. Rapid determination of CaCO₃ in mixtures using FT-IR spectroscopy. Miner. Eng. 14:1107–1111. doi:10.1016/S0892-6875(01)00116-9
- Lucas, S.T., and R.R. Weil. 2012. Can a labile carbon test be used to predict crop responses to improve soil organic matter management? Agron. J. 104:1160–1170. doi:10.2134/agronj2011.0415
- Madari, B.E., J.B. Reeves, M.R. Coelho, P.L.O.A. Machado, and H. De-Polli. 2005. Mid- and near-infrared spectroscopic determination of carbon in a diverse set of soils from the Brazilian National Soil Collection. Spectrosc. Lett. 38:721–740. doi:10.1080/00387010500315876
- Madejová, J. 2003. FTIR techniques in clay mineral studies. Vib. Spectrosc. 31:1–10. doi:10.1016/S0924-2031(02)00065-6
- Margenot, A.J., F.J. Calderón, T.M. Bowles, S.J. Parikh, and L.E. Jackson. 2015. Soil organic matter functional group composition in relation to organic carbon, nitrogen, and phosphorus fractions in organically managed tomato fields. Soil Sci. Soc. Am. J. 79:772–782. doi:10.2136/sssaj2015.02.0070
- Martens, H., and T. Naes. 1989. Multivariate calibration. John Wiley & Sons, Chichester, UK.
- Minasny, B., G. Tranter, A.B. McBratney, D.M. Brough, and B.W. Murphy. 2009. Regional transferability of midinfrared diffuse reflectance spectroscopic prediction for soil chemical properties. Geoderma 153:155–162. doi:10.1016/j.geoderma.2009.07.021
- Nguyen, T.T., L.J. Janik, and M. Raupach. 1991. Diffuse reflectance infrared Fourier-transform drift- Spectroscopy in soil studies. Aust. J. Soil Res. 29:49–67. doi:10.1071/SR9910049
- Panettieri, M., A.E. Berns, H. Knicker, J.M. Murillo, and E. Madejón. 2015. Evaluation of seasonal variability of soil biogeochemical properties in aggregate-size fractioned soil under different tillages. Soil Tillage Res. 151:39–49. doi:10.1016/j.still.2015.02.008
- Parikh, S.J., K.W. Goyne, A.J. Margenot, F.N.D. Mukome, and F.J. Calderón. 2014. Soil chemical insights provided through vibrational spectroscopy. Adv. Agron. 126:1–148. doi:10.1016/B978-0-12-800132-5.00001-8
- Peltre, C., S. Bruun, C. Du, I.K. Thomsen, and L.S. Jensen. 2014. Assessing soil constituents and labile soil organic carbon by mid-infrared photoacoustic spectroscopy. Soil Biol. Biochem. 77:41–50. doi:10.1016/j.soilbio.2014.06.022
- Plaza-Bonilla, D., J. Álvaro-Fuentes, and C. Cantero-Martínez. 2014. Identifying soil organic carbon fractions sensitive to agricultural management practices. Soil Tillage Res. 139:19–22. doi:10.1016/j.still.2014.01.006
- Reeves, J.B. 2003. Mid-infrared diffuse reflectance spectroscopy: Is sample dilution with KBr necessary, and if so, when? Am. Lab. 35:24–28.
- Reeves, J.B. 2010. Near- versus mid-infrared diffuse reflectance spectroscopy for soil analysis emphasizing carbon and laboratory versus on-site analysis: Where are we and what needs to be done? Geoderma 158:3–14. doi:10.1016/j.geoderma.2009.04.005
- Reeves, J.B. 2012. Mid-infrared spectral interpretation of soils: Is it practical or accurate? Geoderma 189-190:508–513. doi:10.1016/j.geoderma.2012.06.008
- Reeves, J.B., R.F. Follett, G.W. McCarty, and J.M. Kimble. 2006. Can near or mid-infrared diffuse reflectance spectroscopy be used to determine soil carbon pools? Commun. Soil Sci. Plant Anal. 37:2307–2325. doi:10.1080/00103620600819461
- Reeves, J.B., G.W. McCarty, and V.B. Reeves. 2001. Mid-infrared diffuse reflectance spectroscopy for the quantitative analysis of agricultural soils. J. Agric. Food Chem. 49:766–772. doi:10.1021/jf0011283
- Reeves, J.B., and D.B. Smith. 2009. The potential of mid- and near-infrared diffuse reflectance spectroscopy for determining major- and trace-element concentrations in soils from a geochemical survey of North America. Appl. Geochem. 24:1472–1481. doi:10.1016/j.apgeochem.2009.04.017
- Reeves, J.B., G.W. McCarty, F.J. Calderón, and W.D. Hively. 2012. Advances in spectroscopic methods for quantifying soil carbon. Elsevier, Waltham, MA. doi:10.1016/B978-0-12-386897-8.00020-6
- Schipanski, M.E., and L.E. Drinkwater. 2011. Nitrogen fixation of red clover interseeded with winter cereals across a management-induced fertility gradient. Nutr. Cycl. Agroecosyst. 90:105–119. doi:10.1007/s10705-010-9415-z
- Schipanski, M.E., L.E. Drinkwater, and M.P. Russelle. 2010. Understanding the variability in soybean nitrogen # xation across agroecosystems. Plant Soil 329:379–397. doi:10.1007/s11104-009-0165-0
- Six, J., R.T. Conant, E.A. Paul, and K. Paustian. 2002. Stabilization mechanisms of soil organic matter: Implications for C saturation of soils. Plant Soil 241:155–176. doi:10.1023/A:1016125726789
- Snapp, S.S., L.E. Gentry, and R. Harwood. 2010. Management intensity– not biodiversity–the driver of ecosystem services in a long-term row crop experiment. Agric. Ecosyst. Environ. 138:242–248. doi:10.1016/j.agee.2010.05.005
- Soriano-Disla, J.M., L.J. Janik, R.A. Viscarra Rossel, L.M. Macdonald, and M.J. McLaughlin. 2014. The performance of visible, near-, and mid-infrared reflectance spectroscopy for prediction of soil physical, chemical, and biological properties. Appl. Spectrosc. Rev. 49:139–186. doi:10.1080/05704928.2013.811081
- Stenberg, B., R.A. Viscarra Rossel, A.M. Mouazen, and J. Wetterlind. 2010. Visible and near infrared spectroscopy in soil science. Adv. Agron. 107:163–215. doi:10.1016/S0065-2113(10)07005-7
- Thomsen, I.K., S. Bruun, L.S. Jensen, and B.T. Christensen. 2009. Assessing soil carbon lability by near infrared spectroscopy and NaOCl oxidation. Soil

- Biol. Biochem. 41:2170–2177. doi:10.1016/j.soilbio.2009.08.002
- Veum, K.S., K.W. Goyne, R.J. Kremer, R.J. Miles, and K.A. Sudduth. 2014. Biological indicators of soil quality and soil organic matter characteristics in an agricultural management continuum. *Biogeochemistry* 117:81–99. doi:10.1007/s10533-013-9868-7
- Viscarra Rossel, R.A., and T. Behrens. 2010. Using data mining to model and interpret soil diffuse reflectance spectra. *Geoderma* 158:46–54. doi:10.1016/j.geoderma.2009.12.025
- Viscarra Rossel, R.A., D.J.J. Walvoort, A.B. McBratney, L.J. Janik, and J.O. Skjemstad. 2006. Visible, near infrared, mid infrared or combined diffuse reflectance spectroscopy for simultaneous assessment of various soil properties. *Geoderma* 131:59–75. doi:10.1016/j.geoderma.2005.03.007
- Wang, F., Y. Tong, P. Gao, J. Zhang, R.R. Weil, and J.N. Coffie. 2014. Organic amendments to a wheat crop alter soil aggregation and labile carbon on the loess plateau, China. *Soil Sci.* 179:166–173. doi:10.1097/SS.0000000000000049
- Weil, R.R., R.I. Kandikar, M.A. Stine, J.B. Gruver, and S.E. Samson-Liebig. 2003. Estimating active carbon for soil quality assessment: A simplified method for laboratory and field use. *Am. J. Altern. Agric.* 18:3–17. doi:10.1079/AJAA2003003
- Wetterlind, J., B. Stenberg, and M. Soderstrom. 2010. Increased sample point density in farm soil mapping by local calibration of visible and near infrared prediction models. *Geoderma* 156:152–160. doi:10.1016/j.geoderma.2010.02.012
- Xiang, H., L. Zhang, and D. Wen. 2015. Change of Soil Carbon Fractions and Water-Stable Aggregates in a Forest Ecosystem Succession in South China. *Forests* 6:2703–2718. doi:10.3390/f6082703